basic computational cost of GPR is $O(n^3)$ [12], due to the fact that an $n \times n$ matrix needs to be inverted for both the gradient calculations required for hyperparameter optimization [12, eq. (5.9)]; and inference (13). This computational expense may become prohibitive for large n. In contrast, even though hyperparameter optimization under BSVR likewise requires matrix inversion for computing the gradient of the evidence [11, eqs. (39)–(41)]), this involves the $m \times m$ matrix Σ_M (cf. (12)), where m usually is considerably smaller than n [11]. To make predictions, BSVR does not require matrix inversion, but rather solving of the convex quadratic optimization problem (10), for which multiple efficient techniques exist [7]. Second, the sparseness property of BSVR can be used towards adaptive data selection when training data is expensive to generate. The sparseness property alludes to the fact that the predictive function can be expressed as a weighted sum of kernel functions centered at the support vectors (SVs), where the SVs are a (usually significantly) reduced subset of the training input vectors. Suppose that a "coarse" regression model using many inexpensive coarsely simulated training data points is set up, and that SVs are identified. It has been shown that the SVs, re-simulated at a high meshing density, can form a sufficient training set for an accurate "fine" model [17]—resulting in substantial computational savings compared to when the full original training set is simulated at the high meshing density. Finally, BSVR's soft insensitive loss function (9) is not overly sensitive to outliers that might arise if training data were obtained from noisy measurements. In contrast, outliers contribute disproportionally to the quadratic loss function in GPR—to the extent that relatively few outliers could adversely affect the solution [11].

It is anticipated that BSVR might be applied with good effect to other antenna-related regression problems that involve non-linear input-output relationships and multi-dimensional inputs.

REFERENCES

[1] Y. Kim, S. Keely, J. Ghosh, and H. Ling, "Application of artificial neural networks to broadband antenna design based on a parametric frequency model," *IEEE Trans. Antennas Propag.*, vol. 55, pp. 669–674, 2007.

[2] G. Angiulli, M. Cacciola, and M. Versaci, "Microwave devices and antennas modelling by support vector regression machines," *IEEE Trans. Magn.*, vol. 43, pp. 1589–1592, 2007.

[3] N. Chauhan, A. Mittal, and M. V. Kartikeyan, "Support vector driven genetic algorithm for the design of circular polarized microstrip antenna," *Int J Infrared Millim. Waves*, vol. 29, pp. 558–569, 2008.

[4] F. Gunes, N. T. Tokan, and F. Gurgen, "A consensual modeling of the expert systems applied to microwave devices," *Int. J. RF Microw. Comput.-Aided Engrg.*, vol. 20, pp. 430–440, 2010.

[5] F. Gunes, N. T. Tokan, and F. Gurgen, "A knowledge-based support vector synthesis of the transmission lines for use in microwave integrated circuits," *Expert Syst. Appl.*, vol. 37, pp. 3302–3309, 2010.

[6] L. Xia, J. C. Meng, R. M. Xu, B. Yan, and Y. C. Guo, "Modeling of 3-D vertical interconnect using support vector machine regression," *IEEE Microw. Wireless Compon. Lett.*, vol. 16, pp. 639–641, 2006.

[7] B. Schölkopf and A. J. Smola, *Learning With Kernels: Support Vector Machines, Regularization, Optimization, and Beyond*. Cambridge, MA: MIT Press, 2002.

[8] M. Martinez-Ramon, J. L. Rojo-Alvarez, G. Camps-Valls, and C. G. Christodoulou, "Kernel antenna array processing," *IEEE Trans. Antennas Propag.*, vol. 55, pp. 642–650, 2007.

[9] A. Randazzo, M. A. Abou-Khousa, M. Pastorino, and R. Zoughi, "Direction of arrival estimation based on support vector regression: Experimental validation and comparison with MUSIC," *IEEE Antennas Wireless Propag. Lett.*, vol. 6, pp. 379–382, 2007.

[10] C. C. Chang and C. J. Lin, LIBSVM: A Library for Support Vector Machines 2001.

[11] W. Chu, S. S. Keerthi, and C. J. Ong, "Bayesian support vector regression using a unified loss function," *IEEE Trans. Neural Netw.*, vol. 15, pp. 29–44, 2004.

[12] C. E. Rasmussen and C. K. I. Williams, *Gaussian Processes for Machine Learning*. Cambridge, MA: MIT Press, 2006.

[13] H. D. Chen, "Broadband CPW-fed square slot antennas with a widened tuning stub," *IEEE Trans. Antennas Propag.*, vol. 51, pp. 1982–1986, 2003.

[14] R. Chair, A. A. Kishk, and K. F. Lee, "Ultrawide-band coplanar waveguide-fed rectangular slot antenna," *IEEE Antennas Wireless Propag. Lett.*, vol. 3, pp. 227–229, 2004.

[15] J. P. Jacobs and J. P. De Villiers, "Gaussian-process-regression-based design of ultrawide-band and dual-band CPW-fed slot antennas," *J. Electromagn. Waves Applicat.*, vol. 24, pp. 1763–1772, 2010.

[16] Zeland Software, IE3D User's Manual vol. 14, 2007.

[17] N. T. Tokan and F. Gunes, "Knowledge-based support vector synthesis of the microstrip lines," *Progr. Electromagn. Res.*, vol. 92, pp. 65–77, 2009.

Dispersive Periodic Boundary Conditions for Finite-Difference Time-Domain Method

Khaled ElMahgoub, Atef Z. Elsherbeni, and Fan Yang

***Abstract*—A dispersive periodic boundary condition (DPBC) is developed for the finite-difference time-domain method to analyze periodic structures with dispersive media on the boundaries of a unit cell. The formulation is based on the auxiliary differential equation (ADE) method with a two-term Debye model and the constant horizontal wavenumber approach. The developed formulation is easy to implement and is efficient in both memory usage and computational time. The validity of this formulation is verified through several numerical examples such as infinite dispersive slab and sandwiched composite frequency selective surface (FSS) structure.**

***Index Terms*—Auxiliary differential equation, Debye model, dispersive media, finite-difference time-domain (FDTD), periodic boundary conditions (PBC).**

I. INTRODUCTION

Periodic structures are of great importance in electromagnetics due to their wide range of applications. The finite-difference time-domain (FDTD) technique has been utilized to analyze these structures, and various periodic boundary conditions (PBC) have been developed such that the computations are performed on only one unit cell instead of the entire structure [1]. Meanwhile, simulation of dispersive media is essential in many applications such as medical telemetries, metamaterials designs, nano plasmonic solar cells, and shielding materials. FDTD also provides an efficient means to simulate these media, and various methods have been developed to model the frequency dependence of the material parameters. The recursive convolution (RC) method [2] and the auxiliary differential equation (ADE) method [3] are the two

Manuscript received March 24, 2011; revised July 31, 2011; accepted September 26, 2011. Date of publication January 31, 2012; date of current version April 06, 2012.

K. ElMahgoub and A. Z. Elsherbeni are with the Center of Applied Electromagnetic System Research (CAESR), Department of Electrical Engineering, University of Mississippi, University, MS 38677 USA (e-mail: kelmahgoub@ieee.org; atef@olemiss.edu).

F. Yang is with the Center of Applied Electromagnetic System Research (CAESR), Department of Electrical Engineering, University of Mississippi, University, MS 38677 USA and also with the Department of Electronic Engineering, Tsinghua University, Beijing, 100084, China (e-mail: fyang@olemiss.edu).

Color versions of one or more of the figures in this communication are available online at http://ieeexplore.ieee.org.

Digital Object Identifier 10.1109/TAP.2012.2186243

most well known approaches. The piecewise linear recursive convolution [4] and the Z-transform [5] are also used to model the dispersive media.

It's worthwhile to point out that most of the previous PBCs for FDTD technique are developed to analyze periodic structures where dispersive materials are not located on the boundary of the unit cells. However, there are numerous applications where dispersive media exist on the boundaries of a unit cell. In this communication, a dispersive periodic boundary condition (DPBC) for the FDTD technique is developed to solve the above challenge. The algorithm is based on the ADE technique with a two-term Debye relaxation equation to simulate general dispersive media. In addition, the constant horizontal wavenumber approach [6]–[9] is modified accordingly to implement the PBCs. Compared to other FDTD/PBC techniques such as field transformation methods, the constant horizontal wavenumber algorithm offers many advantages, including the implementation simplicity and good stability condition for incidences near grazing angles [7].

The communication is organized as follows: In Section II, brief descriptions of the ADE technique and the constant horizontal wavenumber approach are provided, FDTD updating equations are derived, and the DPBC is described. In Section III, numerical examples proving the validity of the approach are presented. Section IV provides the conclusion.

II. Dispersive Periodic Boundary Conditions

In this section an algorithm to implement the DPBC in FDTD is developed. The algorithm is based on the ADE method and the constant horizontal wavenumber approach.

A. Auxiliary Differential Equation Approach

In the ADE method, an additional differential equation relating the electric displacement vector D to the electric field vector E is used in addition to Maxwell's equations. For a dispersive material, the electric displacement vector can be written as

$$D(\omega) = \varepsilon(\omega)E(\omega) \tag{1}$$

where ε is the permittivity. The dispersive characteristics of $\varepsilon(\omega)$ can be described by a two-term Debye relaxation equation as

$$\varepsilon(\omega) = \varepsilon_o \left[\varepsilon_\infty + \frac{\varepsilon_{s1} - \varepsilon_\infty}{1 + j\omega\tau_1} + \frac{\varepsilon_{s2} - \varepsilon_\infty}{1 + j\omega\tau_2}\right] \tag{2}$$

where ε_o is the free space permittivity, ε_{s1} and ε_{s2} are the static relative permittivities, ε_∞ is the relative permittivity at infinite frequency, and τ_1 and τ_2 are the relaxation times. From (1) and (2) $D(\omega)$ can be written as follows:

$$D(\omega) = \varepsilon_o \frac{\varepsilon_s + j\omega(\varepsilon_{s1}\tau_2 + \varepsilon_{s2}\tau_1) - \omega^2\tau_1\tau_2\varepsilon_\infty}{1 + j\omega(\tau_1 + \tau_2) - \omega^2\tau_1\tau_2} E(\omega) \tag{3}$$

where $\varepsilon_s = \varepsilon_{s1} + \varepsilon_{s2} - \varepsilon_\infty$. Equation (3) is a frequency-domain equation of D, and it can be transformed to the following time-domain differential equation

$$\begin{aligned} &D(t) + (\tau_1 + \tau_2)\frac{\partial D(t)}{\partial t} + \tau_1\tau_2\frac{\partial^2 D(t)}{\partial t^2} \\ &= \varepsilon_o\varepsilon_s E(t) + \varepsilon_o(\varepsilon_{s1}\tau_2 + \varepsilon_{s2}\tau_1)\frac{\partial E(t)}{\partial t} + \tau_1\tau_2\varepsilon_o\varepsilon_\infty\frac{\partial^2 E(t)}{\partial t^2}. \end{aligned} \tag{4}$$

Solving this additional (4) simultaneously with the Maxwell's equations will lead to simulating the dispersive property of the medium [10].

B. Constant Horizontal Wavenumber Approach

For periodic structure with periodicity P_x along the x-direction, the PBC of the electric field in frequency domain can be written according to Floquet theory as

$$E(x = 0, y, z, \omega) = E(x = P_x, y, z, \omega) \times e^{jk_x P_x} \tag{5}$$

where

$$k_x = k_0 \sin\theta = \frac{2\pi f}{c}\sin\theta \tag{6}$$

and c is wave velocity in free speed.

Instead of fixing the incidence angle θ, the constant horizontal wavenumber approach fixes the value of the horizontal wavenumber k_x in FDTD simulation. Thus, the term $e^{jk_x P_x}$ is constant in (5). Using a direct frequency domain to time domain transformation, the electric field in time domain can be represented as follows:

$$E(x = 0, y, z, t) = E(x = P_x, y, z, t) \times e^{jk_x P_x}. \tag{7}$$

In this approach, conventional Yee's scheme [11] is used to update the E and H fields, which offer several advantages such as: implementation simplicity, the same stability condition and numerical errors as conventional FDTD [6]. Thus, the constant horizontal wavenumber approach is a good choice for the periodic structure analysis. More details about the approach could be found in [6].

C. The FDTD/DPBC Algorithm

The computational domain is shown in Fig. 1. Different to the conventional FDTD method, the proposed algorithm uses the ADE technique to update the non-boundary electric field components. In addition, a modified version of the constant horizontal wavenumber approach is derived to update electric field components on the boundaries. The algorithm can be summarized as follows.

1. Update H from E using conventional FDTD;
2. Update D from H (non-boundary components) using the ADE technique;
3. Update D from H (boundary components) using DPBC;
4. Update E from D using the ADE technique.

Steps 1, 2 and 4 do not need any further modification compared to the conventional FDTD and the ADE technique. Only for step 3, the constant horizontal wavenumber approach should be modified to include the dispersive feature on the boundary.

The Floquet theory in frequency domain is represented as follows:

$$E(x, y = 0, z, \omega) = E(x, y = P_y, z, \omega) \times e^{jk_y P_y}. \tag{8}$$

Multiplying both sides of (8) by the complex permittivity will result in the following equation:

$$D(x, y = 0, z, \omega) = D(x, y = P_y, z, \omega) \times e^{jk_y P_y}. \tag{9}$$

Equation (9) represents Floquet theory for the displacement electric field vector D. Using the constant horizontal wavenumber approach, (9) can be directly transformed to the time domain as follows:

$$D(x, y = 0, z, t) = D(x, y = P_y, z, t) \times e^{jk_y P_y}. \tag{10}$$

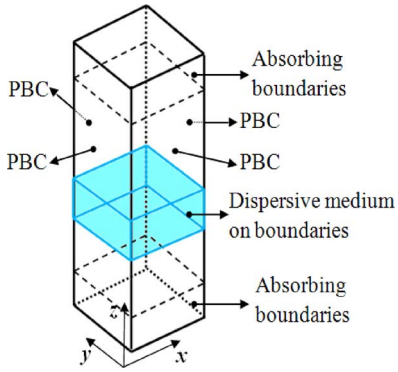

Fig. 1. Computational domain (unit cell geometry).

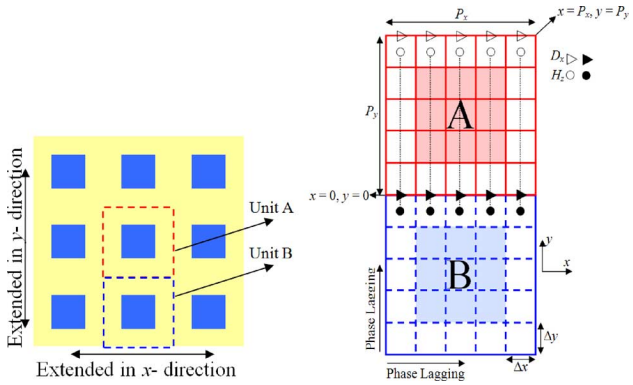

Fig. 2. Geometry of a general periodic structure.

For the x-direction, the updating equation for the D components on the boundary ($y = 0$) can be written as follows:

$$D_x^{n+1}(i,1,k) = D_x^n(i,1,k) + \frac{\Delta t}{\Delta y} \times [H_z^{n+1/2}(i,1,k) - H_z^{n+1/2}(i,0,k)] - \frac{\Delta t}{\Delta z} \times [H_y^{n+1/2}(i,1,k) - H_y^{n+1/2}(i,1,k-1)] \quad (11)$$

where Δy, Δz are the unit cell size in y- and z-directions respectively, and Δt is the time step. From (11) it can be noticed that updating the D components on the boundary ($y = 0$) need the knowledge of magnetic field components outside our unit cell of interest (unit A in Fig. 2). However, due to the periodicity and using the Floquet theory, the magnetic field components H_z inside the unit A can be used to replace the outside magnetic field component as follows:

$$H_z^{n+1/2}(i,0,k) = H_z^{n+1/2}(i,n_y,k) \times e^{jk_yP_y} \quad (12)$$

where n_y is the total number of FDTD cell in the y-direction. Using (11) and (12), all the displacement electric field vectors on the boundary ($y = 0$) can be updated. As for the boundary ($y = P_y$) the updating equation can be represented as follows:

$$D_x^{n+1}(i,n_y+1,k) = D_x^{n+1}(i,1,k) \times e^{-jk_yP_y}. \quad (13)$$

Similar to the x-direction, all the fields in both the y- and z- directions can be updated. The FDTD/DPBC algorithm can also be easily extended to implement dispersive permeability media. In addition, it can be simply used with other dispersive models such as the Lorentz and Drude models. Also, the DPBC can be used with other dispersive simulation techniques such as the RC and Z-transform methods.

III. Numerical Results

In this section, numerical results generated using the FDTD/DPBC algorithm are presented. The FDTD code was developed using MATLAB [12] and executed on a computer with an Intel Core-2 2.66 GHz with 2 GB RAM. These results demonstrate the validity of the algorithm by determining reflection and transmission properties of periodic structures with general dispersive media. The results are compared with results obtained from analytical solution and Ansoft high frequency structural simulator (HFSS) which is based on the finite element method (FEM) [13].

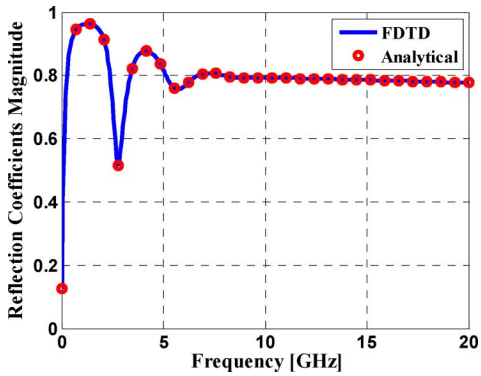

Fig. 3. Reflection coefficient for infinite water slab of thickness 6 mm under normal incidence ($k_x = 0\ \mathrm{m}^{-1}$).

A. An Infinite Water Slab

The algorithm is first used to analyze an infinite water slab with a thickness of 6 mm. The slab is illuminated by TM^z and TE^z plane waves in two different simulations. The parameters of water permittivity are obtained from [10] as: $\varepsilon_{s1} = 81$, $\varepsilon_{s2} = 1.8$, $\varepsilon_\infty = 1.8$, $\tau_1 = 9.4 \times 10^{-12}$ and $\tau_2 = 0$. The geometry of the slab is shown in Fig. 1. The FDTD grid cell size is $\Delta x = \Delta y = \Delta z = 0.125$ mm, and the slab is represented by 2×2 cells (due to the homogeneity of the infinite slab, it can be considered as a periodic structure with any periodicity). In the FDTD code 10,000 time steps are used. Convolutional Perfect Matched Layer (CPML) is used as the absorbing boundaries at the top and the bottom of the computational domain as implemented in [14]. The slab is excited using a cosine modulated Gaussian pulse centered at 10 GHz and with a 20 GHz bandwidth for the normal incident case ($k_x = 0\ \mathrm{m}^{-1}$), and it is excited using a cosine modulated Gaussian pulse centered at 12.75 GHz and with a 14.5 GHz bandwidth for the oblique incident case ($k_x = 104.8\ \mathrm{m}^{-1}$). Here, the bandwidth is defined as the frequency band where the magnitude of the excitation decays to 10% of its maximum. The angle span for $k_x = 104.8\ \mathrm{m}^{-1}$ and the frequency range from 5.5 to 20 GHz is from 65.5° to 14.5°. The results are compared with analytical results. From Figs. 3 and 4, good agreements between analytical solutions and FDTD results can be noticed for both TM^z and TE^z cases (normal and oblique incidence).

B. Sandwiched Composite FSS

The algorithm is then used to analyze a sandwich composite-FSS structure. The composite materials have been investigated for their potential applications as shielding materials to protect electronics system from electromagnetic pulse or electromagnetic interferences.

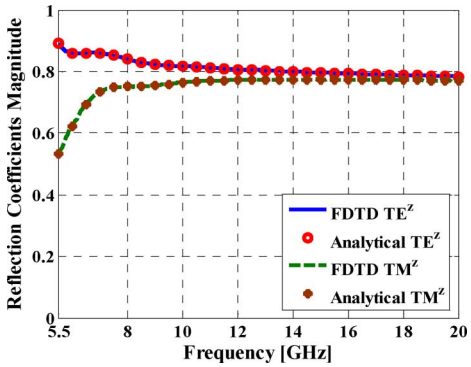

Fig. 4. Reflection coefficients for infinite water slab of thickness 6 mm under TM^z and TE^z oblique incidence ($k_x = 104.8\ \mathrm{m}^{-1}$).

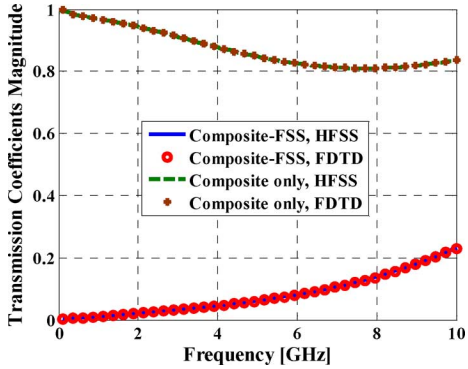

Fig. 6. Transmission coefficient for sandwiched composite-FSS structure under normal incident TE^z plane wave ($\theta = 0°$, $\varphi = 0°$).

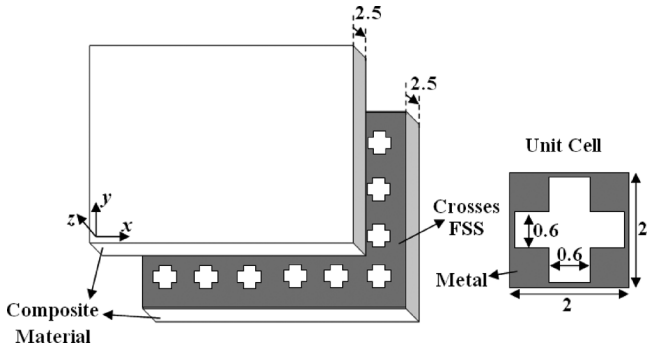

Fig. 5. Geometry of the sandwiched composite-FSS structure (all dimensions are in mm).

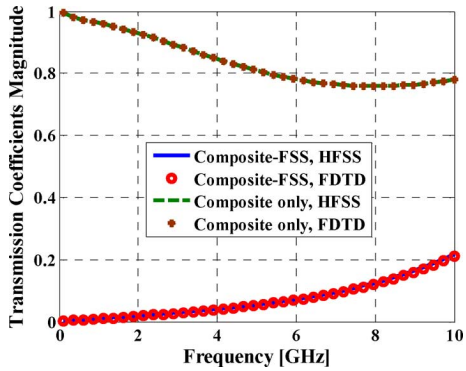

Fig. 7. Transmission coefficient for sandwiched composite-FSS structure under oblique incident TE^z plane wave ($\theta = 30°$, $\varphi = 60°$).

To enhance the shielding effectiveness, one possible solution is to introduce additional layer or layers of FSS structures between the interfaces of composite materials [15]. The sandwiched structure studied here is shown in Fig. 5. An infinite thin metal film is inserted between two composite material layers with a thickness of 2.5 mm each, the metal film has a periodic array of cross-shaped slots with a 2 mm periodicity in both x- and y-directions. The parameters of the permittivity of composite medium can be stated as [14]: $\tau_{s1} = 5.2$, $\varepsilon_{s2} = 3.7$, $\varepsilon_\infty = 3.7$, $\tau_1 = 5.27 \times 10^{-10}$ and $\tau_2 = 0$. The structure is simulated using FDTD grid cell size $\Delta x = \Delta y = \Delta z = 0.1$ mm, and CPML is used as the absorbing boundaries at the top and the bottom of the computational domain.

The structure is first illuminated by a normally incident TE^z plane wave ($\theta = 0°$ and $\varphi = 0°$) using a cosine modulated Gaussian pulse centered at 5 GHz with a bandwidth of 10 GHz. Then the structure is illuminated by an obliquely incident TE^z plane wave ($\theta = 30°$ and $\varphi = 60°$). Multiple runs of the code are needed to generate results for many frequencies and a specific oblique incident angle. To study the shielding enhancement provided by adding the FSS layer, the transmission coefficient without the presence of the FSS is provided as a reference.

Fig. 6 provides results for a normal incidence ($\theta = 0°$ and $\varphi = 0°$). Good agreement can be noticed between the FDTD/DPBC results and the HFSS results. The computational time for FDTD is equal to 9.56 minutes while for HFSS for 40 frequency point the computational time is 12.34 minutes which proves efficiency and validity of the algorithm. Fig. 7 provides results for an oblique incidence ($\theta = 30°$ and $\varphi = 60°$), and good agreement is obtained between FDTD/DPBC and HFSS simulations. The computational time for FDTD is equal to 13.6 minutes while for HFSS the computational time is 14.8 minutes. It could be noticed from Figs. 6 and 7 that the transmission coefficient is dramatically decreased due to the presence of the FSS which enhance the shielding effect.

IV. Conclusion

This communication introduces an FDTD/DPBC algorithm to analyze the scattering properties of periodic structures with dispersive media on the boundaries. The approach is developed based on both the constant horizontal wavenumber technique and the ADE technique. It is simple to implement and efficient in terms of both computational time and memory usage. The algorithm is capable of calculating reflection and transmission coefficients in the case of normal and oblique incidences, for both TE^z and TM^z cases. Numerical examples for potential applications such as dispersive slabs and sandwiched composite FSS were provided. The results show good agreement with results obtained from the analytical solution for a dispersive slab and the frequency domain solutions for a dispersive periodic structure.

References

[1] A. Taflove and S. C. Hagness, *Computational Electrodynamics: The Finite-Difference Time-Domain Method*, 3rd ed. Norwood, MA: Artech House, 2005, ch. 9.

[2] T. Kashiwa and I. Fukai, "A treatment by the FD-TD method of the dispersive characteristics associated with electronic polarization," *Microw. Opt. Technol. Lett.*, vol. 3, no. 6, pp. 203–205, 1990.

[3] R. Luebbers, F. P. Hunsberger, K. S. Kunz, R. B. Standler, and M. Schneider, "A frequency dependent finite difference time domain formulation for dispersive materials," *IEEE Trans. Electromagn. Compat.*, vol. 32, no. 3, pp. 222–227, 1990.

[4] D. F. Kelley and R. J. Luebbers, "Piecewise linear recursive convolution for dispersive media using FDTD," *IEEE Trans. Antennas Propag.*, vol. 44, no. 6, pp. 792–798, 1996.

[5] D. M. Sullivan, "Frequency-dependent FDTD methods using Z transforms," *IEEE Trans. Antennas Propag.*, vol. 40, no. 10, pp. 1223–1230, 1992.
[6] F. Yang, J. Chen, R. Qiang, and A. Z. Elsherbeni, "A simple and efficient FDTD/PBC algorithm for scattering analysis of periodic structures," *Radio Sci.*, vol. 42, p. RS4004, Jul. 2007.
[7] K. ElMahgoub, F. Yang, A. Z. Elsherbeni, V. Demir, and J. Chen, "FDTD analysis of periodic structures with arbitrary skewed grid," *IEEE Trans. Antennas Propag.*, vol. 58, no. 8, pp. 2649–2657, 2010.
[8] K. ElMahgoub, F. Yang, A. Z. Elsherbeni, V. Demir, and J. Chen, "FDTD/PBC algorithm for skewed grid periodic structures," in *Proc. IEEE Antennas and Propagation Society Int. Symp.*, Toronto, ON, Canada, Jul. 11–17, 2010, pp. 1–4.
[9] K. ElMahgoub, A. Z. Elsherbeni, and F. Yang, "Analysis of periodic structures with dispersive material using the FDTD technique," in *Proc. XXXth URSI General Assembly and Scientific Symp.*, Aug. 13–20, 2011, pp. 1–4.
[10] O. P. Gandhi, B. Gao, and J. Y. Chen, "A frequency-dependent finite-difference time-domain formulation for general dispersive media," *IEEE Trans. Microwave Theory Tech.*, vol. 41, no. 4, pp. 658–665, 1993.
[11] K. S. Yee, "Numerical solution of initial boundary value problems involving Maxwell's equations in isotropic media," *IEEE Trans. Antennas Propag.*, vol. 14, pp. 302–307, 1966.
[12] MATLAB Distributed by Mathworks. [Online]. Available: www.mathworks.com
[13] Ansoft HFSS Software is Distributed by the Ansoft Corporation. [Online]. Available: www.ansoft.com/products/hf/hfss/
[14] A. Elsherbeni and V. Demir, *The Finite Difference Time Domain Method for Electromagnetics: With MATLAB Simulations*. New York: SciTech Publishing, 2009.
[15] R. Qiang, J. Chen, J. Huang, M. Koledintseva, E. Dubroff, J. Drewniak, and F. Yang, "Numerical analysis of sandwiched composite-FSS structures," in *Proc. IEEE Int. Symp. Electromagn. Compat.*, 2006, pp. 742–746.

A Memory-Efficient Implementation of TLM-Based Adjoint Sensitivity Analysis

Osman S. Ahmed, Mohamed H. Bakr, and Xun Li

***Abstract*—We present a memory efficient algorithm for the estimation of adjoint sensitivities with the 2D transmission line modeling (TLM) method. The algorithm is based on manipulating the local scattering matrices to reduce the required storage for the original structure simulation associated with lossy dielectric discontinuities. Only one value per cell is stored for two dimensional simulations. Moreover, the connection step for the scattered sensitivity storage is embedded during the adjoint simulation and the sensitivity estimates are calculated on the fly. The required memory storage for our implementation is only 10% of the original implementation of AVM sensitivity with TLM.**

***Index Terms*—Computer-aided design (CAD), transmission line modeling (TLM), adjoint variable method (AVM).**

I. Introduction

Adjoint variable methods (AVM) has opened a way for significant acceleration of derivative-based optimization of microwave structures [1]–[5]. The AVM estimates the sensitivity of the objective function with respect to all parameters using at most one extra simulation. AVM approaches can be contrasted with finite difference approaches where at least N extra simulations are calculated where N is the number of parameters. The AVM approach has been successfully developed for both time and frequency domain numerical techniques [4]–[8]. Recently the AVM algorithm has found early implementation in commercial software such as HFSS [9] and CST [10].

The development of the AVM approach for transmission line modeling (TLM) has been achieved in several stages. The AVM was first developed for 2D time-domain TLM problems with perfect conducting discontinuity where the shape of a metallic object is the optimizable design parameter [3]. An efficient mapping algorithm is developed in order to avoid the simulation of a perturbed adjoint structure. In this approach only the perturbed transmission line links connected to the metallic object needs to be stored.

TLM-based AVM approaches for lossy dielectric discontinuities require huge memory storage during both the original and the adjoint simulation [11]. For these problems, the perturbation is volumetric and thus the entire discontinuity domain is perturbed. All the TLM links inside the dielectrically perturbed domain are stored during the original and adjoint simulation at all time steps.

In this communication, we present a novel memory efficient implementation of the AVM algorithm with TLM. We show that the memory requirement is reduced to only 10% of that required for original 2D TLM-based AVM algorithm [11]. A mathematical manipulation of the

Manuscript received January 28, 2011; revised August 29, 2011; accepted November 05, 2011. Date of publication January 31, 2012; date of current version April 06, 2012. This work was supported in part by the Natural Sciences and Engineering Research Council of Canada (NSERC) Discovery grant (RGPIN 249780-2011).

O. S. Ahmed and M. H. Bakr are with the Computational Electromagnetics Research Laboratory, Department of Electrical and Computer Engineering, McMaster University, Hamilton, ON L8S 4K1, Canada (e-mail: mohammos@mcmaster.ca; mbakr@mail.ece.mcmaster.ca).

X. Li is with the Photonics Research Laboratory, Department of Electrical and Computer Engineering, McMaster University, Hamilton, ON L8S 4K1, Canada (e-mail: lixun@mcmaster.ca).

Color versions of one or more of the figures in this communication are available online at http://ieeexplore.ieee.org.

Digital Object Identifier 10.1109/TAP.2012.2186237